

9th International Conference Interdisciplinarity in Engineering, INTER-ENG 2015, 8-9 October
2015, Tirgu-Mures, Romania

Modeling an Eddy-Current Probe for Damage Detection of Surface Cracks in Metallic Parts

Abdeslam Aoukili^{a,*}, Abdellatif Khamlichi^b

^aDepartment of Physics, FST, University Abdelmalek Essaadi, Tetouan 93030, Morocco

^bDepartment TITM, National School of Applied Sciences at Tetouan, University Abdelmalek Essaadi, Tetouan 93030, Morocco

Abstract

Surface crack detection in metallic parts was considered through modeling the eddy-current pattern induced by a variable magnetic field. This was undertaken by means of the finite element method under harmonic inductive excitation and stationary conditions. The proposed model included the array excitation coils, the array sensing coils, the tested defected plate and the ambient air. A parametric study was conducted then in order to determine the influence of the work frequency and the position of the receiver coil on voltage variation at its bottom edge.

The obtained results have shown that the work frequency has little influence on the results in the investigated range of frequencies. On the opposite the position of the receiver coil was found to have a drastic effect on the voltage variations during scanning. It is then possible to optimize the positions of the receiver coils to provide best sensing in terms of voltage variations when the probe passes over the flaw.

© 2016 The Authors. Published by Elsevier Ltd. This is an open access article under the CC BY-NC-ND license (<http://creativecommons.org/licenses/by-nc-nd/4.0/>).

Peer-review under responsibility of the “Petru Maior” University of Tirgu Mures, Faculty of Engineering

Keywords: crack; metallic parts; eddy-currents; finite element method; numerical simulation.

1. Introduction

Non-destructive evaluation (NDE) techniques based on electromagnetic methods are commonly used for inspection of metallic parts[1]. Some of these inspection methods are based on eddy-currents (EC) which are a

* Corresponding author. Tel.: +212 668152043; fax: +212 539994624.

E-mail address: aoukilia@yahoo.fr

consequence of electromagnetic induction phenomenon. In EC testing, the depth of penetration into the material is controlled by the conductivity of the tested material and the work frequency. Flaws that lie parallel to the probe may not be detectable, so proper orientation of the probes should be arranged.

In the standard configuration of EC testing, a coil carrying alternative sinusoidal current is generally placed in proximity to the specimen. This current generates variable magnetic field which interacts with the test specimen and generates EC. Variations in the phase and magnitude of these EC can be monitored using a second receiver coil or by measuring changes appearing in the current flowing in the primary excitation coil [2,3]. Variations in the electrical conductivity or magnetic permeability of the test object, as well as the existence of a flaw, will cause a change in these EC which in their turn will affect the measured current [4].

The main advantage of EC testing is that they can be used to detect small cracks in or near the surface of the conductive material. The increasing complexity of the structures to be controlled and the augmented needs in terms of capacity of detection, particularly in terms of reachable depth and orientation of flaws as well as on the dynamics of measurement and space resolution, have raised new challenges regarding design of new EC sensors.

To extend the performance of detection in terms of accessible depth, signal-to-noise ratio (SNR) and space resolution, a close understanding of the EC testing system is required. The challenge is in fact about how to determine the optimal distribution of the EC probe providing the best signal indication of the defect. Many parameters enter in the problem and it is necessary to carry out multiple simulations that can resolve the influence of each factor on the quality of the obtained indication.

A great deal of research activity has been dedicated recently to EC inspection based techniques. Some of these contributions include Photo-inductive Imaging (PI) [5], Pulsed Eddy Current (PEC) based methods [6] and Multi-Frequency Eddy Current approaches (MFE) [7].

The various EC based approaches can be improved by exploring new possibilities. The aim is to reach better SNR and to guarantee better resolution with regards to defect detection. Among the perspectives that are actually pursued one can find signal optimization in terms of the frequency interval of work and the design of further smart probes including those of array type [8].

Simulation of EC probes can enhance in fact the development process of advanced measurement devices and methods. Among the important work performed in the context of FEM modelling of EC problems, Mihalache et al. [9] presented a numerical simulation of an EC transducer with orthogonal coils. They developed a 3D numerical analysis based on the magnetic scalar and vector potentials. They used both the standard FEM and the hierarchical FEM of high order and found that the image from the transducer when it passes over a discontinuity is in excellent agreement with 3D theoretical predictions.

Advanced finite element methods using the electric field-based formulations of EC problems have been proposed in Sterz et al. [10]. Rosado et al. [11] have used FEM approach to compute response and to parametrically design several planar EC probes.

Considering the Single-Frequency Eddy Current (SFE) configuration of EC testing, a FEM based model is developed in the following under Comsol software package [12]. The objective is to assess the effect of key parameters on EC defect sensing effectiveness for a homogeneous and isotropic perfect conductive part. This is assumed to be subjected to a stationary induction field created by a series of feed coils. The response of an array of coils sensors is calculated by considering full interaction of diffusion like stationary electromagnetic waves that occurs within this array sensor. The considered parameters include the work frequency and the distance separating the coils from the tested sample. Using a B-scan sweeping protocol, detection of a small defect having the shape of an open cavity is investigated via monitoring the variations affecting the voltage in the receiver coils.

Nomenclature

a_c	transverse section of the coil wire (m^2)
B	inductive magnetic field (T)
B_0	spatial part of the inductive magnetic field (T)
d	air gap between the sensor and the plate (m)
D	electric displacement ($C.m^{-1}$)
E	electric field ($V.m^{-1}$)

E_0	spatial part of the electric field ($V.m^{-1}$)
f	frequency (Hz)
I_c	current magnitude in the coil wire (A)
j	unitary pure imaginary
J	current density ($A.m^{-1}$)
h	height of the plate (m)
h_d	height of the defect (m)
H	magnetic excitation field ($A.m^{-1}$)
ℓ	width of the plate (m)
L	length of the plate (m)
ℓ_d	width of the defect (m)
L_d	length of the defect (m)
t	time (s)
φ_E	initial phase of the electric field (rad)
φ_B	initial phase of the electric field (rad)
ε	permittivity of the medium ($F.m^{-1}$)
μ	permeability of the medium ($H.m^{-1}$)
μ'_r	relativity permeability of copper
ω	radial frequency ($rad.s^{-1}$)
ρ	density of charge ($C.m^{-3}$)
σ	electric conductivity of the medium ($S.m^{-1}$)
σ'	electric conductivity of copper ($S.m^{-1}$)
σ_{air}	electric conductivity of air ($S.m^{-1}$)
Δ	Laplacian operator

2. Analysis and modeling

The constitutive equations governing a perfect Ohmic homogeneous and isotropic conductive medium write

$$J = \sigma E, \quad D = \varepsilon E, \quad B = \mu H \quad (1)$$

In case of a metallic material, the distribution of charges vanishes quickly due to the high conductivity and it is expedient to assume $\rho = 0$. A decoupling happens then in the Maxwell equations and the following propagation-diffusion equations are obtained

$$\Delta E - \varepsilon \mu \frac{\partial^2 E}{\partial t^2} - \mu \sigma \frac{\partial E}{\partial t} = 0, \quad \Delta B - \varepsilon \mu \frac{\partial^2 B}{\partial t^2} - \mu \sigma \frac{\partial B}{\partial t} = 0 \quad (2)$$

A stationary and harmonic solution of equations (2) is such that $E = E_0 e^{j(\omega t - \varphi_E)}$ and $B = B_0 e^{j(\omega t - \varphi_B)}$, where $\omega = 2\pi f$ is the radial frequency and f the frequency of the wave. As for most metals at 20°C, ε is of order $10^{-11} F/m$ and the conductivity is greater than $10^6 S/m$, considering low work frequencies not exceeding $10^3 Hz$ one can verify that the condition $\omega \ll \sigma / \varepsilon$ is satisfied. This enables to simplify equations (2) by neglecting the propagation terms and keeping just the diffusive parts as follows

$$\Delta E_0 - j \mu \omega \sigma E_0 = 0, \quad \Delta B_0 - j \mu \omega \sigma B_0 = 0 \quad (3)$$

Equations (1) and (3) yield the existence of a permanent density of currents that are circulating in the conductive

material and having the form $J = \sigma E_0 e^{j(\omega t - \varphi_E)}$, these compose the EC.

For a given specimen geometry, the field J can be computed by integrating equations (3) under given boundary conditions. In the presence of a singularity or a flaw in the medium, the conductivity varies and the EC distribution will show changes as compared to the pattern associated to the intact geometry. This provides a way of using these EC as indicators to monitor flaw detection in metallic parts.

The practical implementation of this technique of diagnosis sets usually on two circuits. The first one constitutes the inductive part which puts a stationary variable magnetic field in the test material. The second circuit takes the form of a single coil or multiple coils sensor. Figure 1 depicts the EC probe proposed in this work and having the form of an array of coils. These consist of open circuits that are influenced by the variable magnetic field created by the EC inside the test material. The receiver coils can detect voltage perturbations induced by the EC while the compact probe is crossing a zone with variable local conductivity. As a receiver shows high sensitivity only in the immediate proximity of a flaw, using multiple receivers allows for detecting more efficiently EC. Working with greater steps during scanning is then feasible, which will allow to speed up the diagnosis procedure.

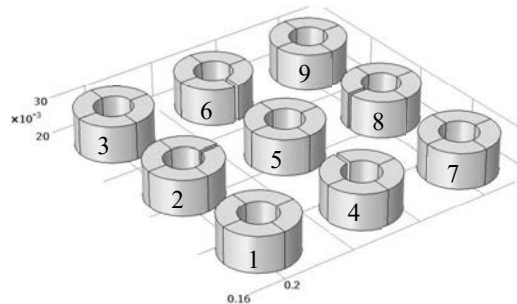


Fig. 1 Details of the EC array sensor; the inductive coils are labelled 1,3,5,7,9 while the receivers coils are labelled 2,4,6 and 8

The material is excited by circulating a sinusoidal current in the inductive coils and an induced voltage is created in the receiver coils which define the sensing parts. This voltage is proportional to the intensity of EC field developing in the skin of the examined part which is a property of high electric conductive materials such as metals.

In practice, the excitation frequency can be monitored to reach deep points of the material, but also the magnitude of the inductive magnetic field B_0 can be increased by using a coil containing a high number of whorls. Working with low frequencies enables to reach more effectively near surface flaws.

For a material with general geometry, solution of equations (3) can be achieved by means of the FEM. In the following Comsol Multiphysics software package [12] is used to simulate the EC device with nine coils as shown in figure 1. Comsol software which provides solutions for multiphysics modeling is based on finite element analysis of various physics and engineering problems, especially in the framework of coupled phenomena. In addition to conventional physics-based user interfaces, Comsol Multiphysics also allows for entering coupled systems of partial differential equations (PDEs) such as equations (3). The PDEs can be entered directly or by using the so-called weak form. This can be done also for the appropriate boundary conditions intervening in the actual problem. Several add-on products are available for COMSOL Multiphysics. These have been categorized according to the applications areas. Here, use is made of the AC/DC Module which is available for simulating electric, magnetic, and electromagnetic fields in static and low-frequency applications.

3. Results and discussion

Let's consider a rectangular plate made from aluminium with length $L=800mm$, width $\ell=400mm$ and depth $h=10mm$, figure 2. The plate material characteristics are $\sigma=3.774 \times 10^7 S.m^{-1}$ and $\mu_r=1H.m^{-1}$. A defect having the form of an open parallelepiped cavity that has sides parallel to those of the plate is assumed to be present at the center of the plate. Its dimensions are taken to be: $L_d=20mm$, $\ell_d=20mm$ and $h_d=5mm$.

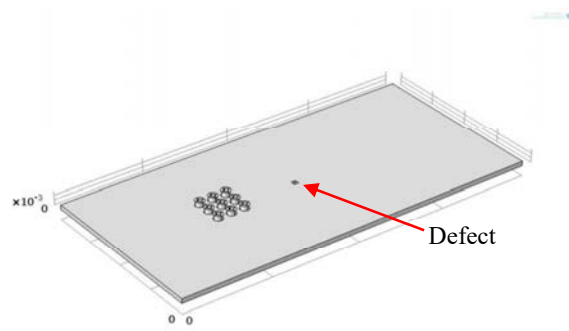


Fig. 2 The test plate sample model geometry

The inductive coils are made from copper for which $\sigma' = 6 \times 10^7 \text{ S.m}^{-1}$ and $\mu'_r = 1 \text{ H.m}^{-1}$. The coil base is circular with radius 10 mm . This coil is assumed to be formed by 1000 whorls having the section area $a_c = 10^{-6} \text{ m}^2$. It is assumed to be crossed by a circulating sinusoidal current of magnitude $I_c = 1 \text{ A}$. The sensor coils which correspond to those labelled 2,4,6 and 8 in figure 1, are made also from copper. The open form of these coils enables to measure the voltage between any pair of points placed on their blades. The base of receiver coils is circular with the same diameter than that of the inductive coils.

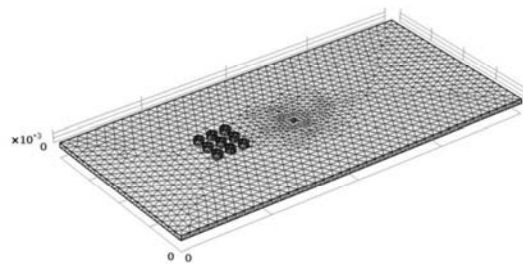


Fig. 3 The finite element mesh used for the plate and the coils

A FEM model was developed for the system. Fig. 3 gives the obtained mesh at convergence. The mesh was generated automatically by using free tetrahedral elements under Comsol. The nine elements constituting the probe-coil setup are meshed using the same element type; the maximum size was fixed at 20 mm for the plate and 10 mm for the coils.

As the excitation coils are coupled to the test specimen through air according to equations (3), the environmental air should also be meshed. Because meshing an infinite volume is not possible, it is necessary to specify a finite volume to mesh and solve for it. In the present study, the whole probe-coil setup was placed at the centre of a cube as shown in Fig. 4. To avoid reflection that is susceptible to take place in a finite volume domain, the default boundary condition corresponding to magnetic insulation is used at the cube boundaries. This condition forces the field to be tangential to the exterior boundaries. The cube used in the present model has a length side of 2000 mm . The air electric conductivity is fixed at $\sigma_{\text{air}} = 10 \text{ S.m}^{-1}$.

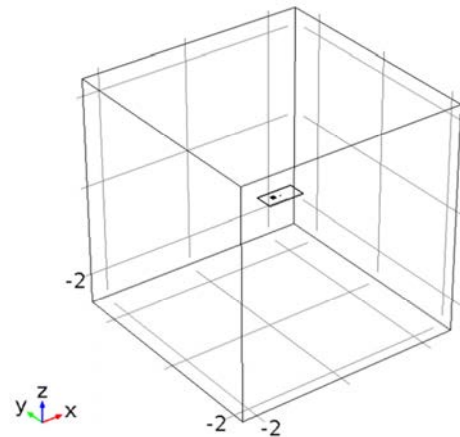


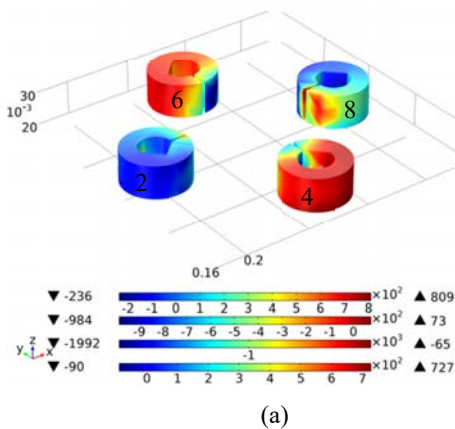
Fig. 4 The complete model of the EC probe setup and test specimen

Three work frequencies are selected: $f_1=50\text{Hz}$, $f_2=100\text{Hz}$ and $f_3=200\text{Hz}$. Both the inductive and the sensor coils are placed at the same distance from the top surface of the plate assumed to be perfectly smooth and planar. The air gap separating the coils from the inspected plate was fixed at $d=50\text{mm}$.

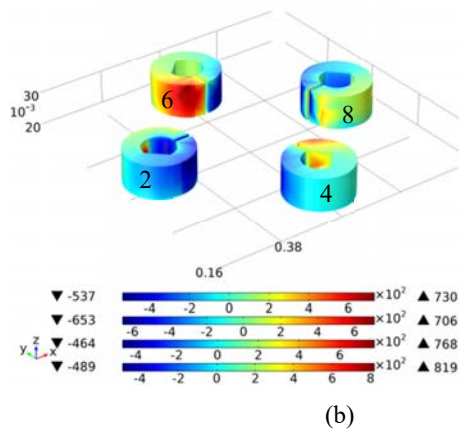
The EC intensities in the receiver coils were calculated by FEM computation. Internal boundary condition corresponding to electric and magnetic surfaces were applied and the density of charge was fixed at zero. Figure 5 shows contours of the y - component of the induced electric field in the receiver coil for both the defect free plate and the defected one.

2- Electric field, y component (V/m) 4- Electric field, y component (V/m)
6- Electric field, y component (V/m) 8- Electric field, y component (V/m)

2- Electric field, y component (V/m) 4- Electric field, y component (V/m)
6- Electric field, y component (V/m) 8- Electric field, y component (V/m)



(a)



(b)

Fig. 5 Contours of the y -component of the induced electric field in the receiver coil; the parameters used are $d=10\text{mm}$ and $f_3=200\text{Hz}$

(a) defect-free plate; (b) defected plate

Considering a cut-line that crosses the defect at its centre as shown in red color in figure 6, four positions of the coils were considered along this line to emulate a basic B-scan. The first position corresponds to the centre placed at

the distance 220mm left from the defect position. The second position corresponds to the centre of the sensor placed right on the defect center, Figure 6.

Figure 7 presents the obtained cut-line of induced current density for the two positions of the coils that are shown in Fig. 6.

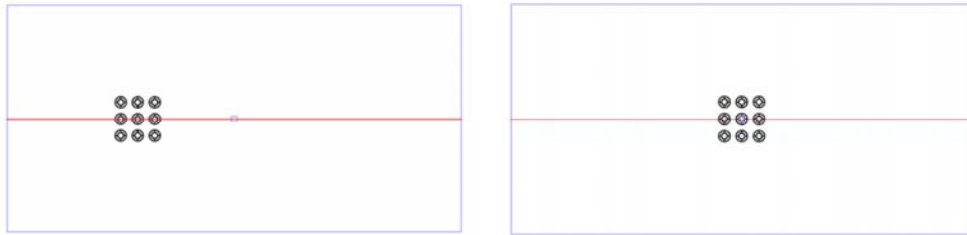


Fig. 6 The two positions of the coils near the flaw considered for the B-scan

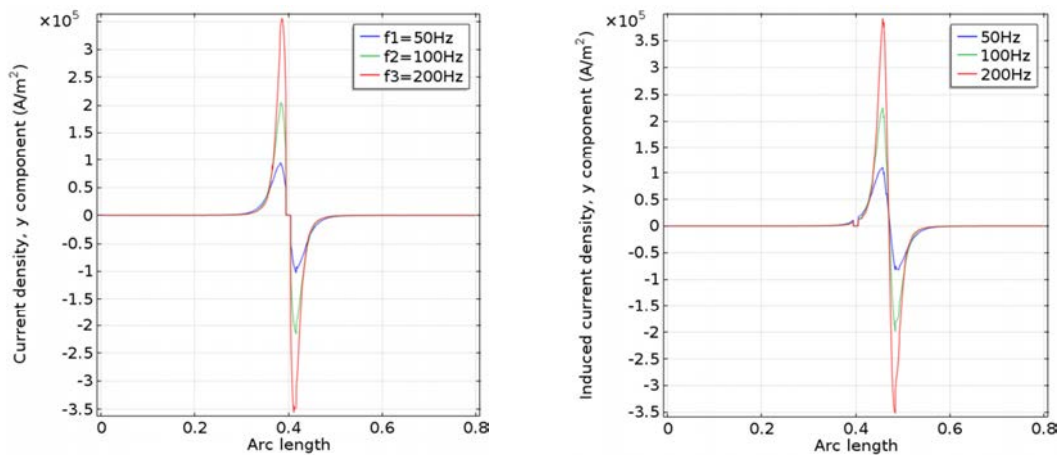


Fig. 7 Cut-lines giving the y-component of induced current density J for the two considered positions of the coils and the three work frequencies when $d=10\text{mm}$ (order of cut-lines is that appearing in Figure 6)

The receiver coils sense the effect resulting from the presence of a flaw in the inspected plate. The receiver blades will show a voltage variation. Connecting a pair of points chosen on these blades with a voltage sensor can be used to monitor the information about defects.

Figure 8 presents, for a given coil, voltage variations between a pair of corners taken symmetrically on the opposite blades at the inner bottom of the coil.

Figure 7 shows that with increasing frequency, the magnitude of EC increases. However for locations close to the defect zone, the three work frequencies give almost the same results.

Figure 8 shows that voltage variations depend on the selected coil. Coil 4 was found to provide the best result as the obtained variations were the highest. It is followed by coil 2, then coil 6, while coil 8 showed reduced variations of voltage. This is quite normal as this last is far from the defect location. The frequency used to obtain the results of Figure 8 is equal to 50Hz. The same results are obtained for the frequency 200Hz, showing that the work frequency has very little influence on the sensed voltage variations.

The simulations presented in this work show that the coils do not provide the same voltage variations while being in the vicinity of a flaw. Using multiple coils offers the possibility to increase the detectability of defects as the presence of a perturbation produced by a flaw could then excite more promptly one of the receiver coils. This is more difficult to occur in the presence of a single coil as this last should be located right on the defect. One can also

mount a circuit by considering association of various pairs of points placed on various coils in order to strengthen the sensing signal in terms of voltage variations. Resolution of flaw detection would then be undoubtedly enhanced.

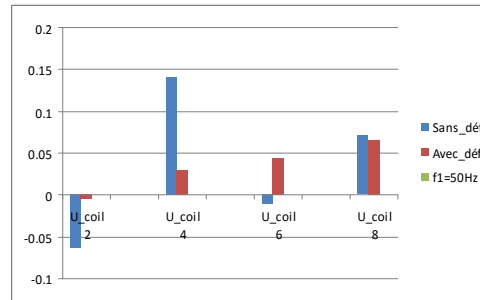


Fig. 8 Voltage variations between a pair of points representing opposite corners of the receiver coil at the bottom of the blades when the sensor is right over the defect; the work frequency used is 50 Hz

This work has shown the possibility of using a multi-coils EC based probe in order to increase sensitivity with regards to flaw detection in metallic parts. The array of coils presented has enabled to get significant voltage variations, which are susceptible to allow then for more accurate indication of the defect. This last can be localized more quickly than for a classical configuration where only one receiver coil is employed.

4. Conclusion

Non destructive evaluation based on eddy-current has been investigated in this work for a multi-coils based probe. Assuming stationary field solution under sinusoidal current excitation, finite element method analysis of the problem was performed by means of Comsol software package. Post-processing of the obtained results has shown that detection of defects can be performed by using the information provided by voltage variations that are experienced at selected points placed on the receiver coil blades. The present analysis has shown that the work frequency has little influence on the results in the investigated range of frequencies. On the opposite the coil position was found to have a huge effect on the voltage variations during scanning. This could be optimized and monitored in order to enhance quality of assessment results provided by eddy-current based techniques.

References

- [1] Rosado L, Gonzalez S, Ramos TG, Vilac PM, Piedade M. A Differential planar eddy currents probe, Fundamentals modeling and experimental evaluation. NDT&E International 2012; 51: 85-93
- [2] Xu P, Huang S, Zhao W. A new differential eddy current testing sensor used for detecting crack, extension direction NDT&E International 2011; 44: 339-343.
- [3] Rahman Ur M. Optimization of in-line defect detection by eddy current techniques, PhD Thesis Kassel University Germany, 2010.
- [4] Rosell A, Persson G. Finite element modelling of closed cracks in eddy current testing, International Journal of Fatigue 2012; 41: 30-38.
- [5] Pan M He Y, Tian G, Chen D, Luo F. Defect characterisation using pulsed eddy current thermography under transmission mode and NDT applications, NDT & E International 2012; 52: 28-36.
- [6] Wilson J W, Tian, GY. Pulsed electromagnetic methods for defect detection and characterisation, NDT&E International 2007; 40: 275-283.
- [7] Bosse Joubert J, Larzabal P-Y, Ferréol PA. High resolution approach for the localization of buried defects in the multi-frequency eddy current imaging of metallic structures, NDT & E International 2010; 43: 250-257
- [8] Grimberg R, Udpa L, Savin A, Steigmann R, Palihovici V, Udpa S. 2D Eddy current sensor array, NDT&E International 2006; 39: 264-271.
- [9] Mihalache O, Grimberg R, Radu E, Savin A. Finite element numerical simulation for eddy current transducer with orthogonal coils, Sensors and Actuators A Physical 1997; 59: 213-218.
- [10] Sterz O, Hauser A, Wittum G. Adaptive local multigrid methods for solving time-harmonic eddy-current problems, IEEE Trans Magnet 2006; 4: 309-318.
- [11] Rosado LS, Gonzalez JC, Santos JC, Ramos TG, Piedade PM. Geometric optimization of a differential planar eddy currents probe for non-destructive testing, Sensors and Actuators A Physical 2013; 197: 96-105.
- [12] ***. Introduction to Comsol Multiphysics, version 4.4 Comsol, Sweden; 2013.